ELSEVIER

Biophysical Chemistry 86 (2000) 15–28

Biophysical Chemistry

www.elsevier.nl/locate/bpc

Effect of Adriamycin on the boundary lipid structure of cytochrome *c* oxidase: pico-second time-resolved fluorescence depolarization studies

Tapan Kanti Das[a], Shyamalava Mazumdar[b,*]

[a] *Albert Einstein College of Medicine, 1300 Morris Park Avenue, Bronx, NY 10461, USA*
[b] *Department of Chemical Sciences, Tata Institute of Fundamental Research Homi Bhabha Road, Mumbai 400005, India*

Received 17 December 1999; received in revised form 5 April 2000; accepted 7 April 2000

Abstract

The fluorescence dynamics of the dye 3,3′-diethyloxadicarbocyanine iodide (DODCI) was used to probe the microenvironment of cytochrome *c* oxidase (C*c*O) and cardiolipin. The dye was partitioned between an aqueous and a hydrophobic phase. The 'bound' and 'free' populations of DODCI could be separated by analysis of the time-resolved fluorescence decay of the dye. The anisotropy decay of the DODCI bound to C*c*O showed a unique 'dip and rise' shape that was analyzed by a combination of rotational correlation times with time-dependent weight factors for each lifetime component. Rotational dynamics studies revealed the existence of a restricted motion of the dye bound at the enzyme surface. Adriamycin, an anticancer, albeit cardiotoxic drug, was previously proposed to affect the surface structure of C*c*O, most likely by causing a disorder to the surface lipid arrangement. A drastic change in the rotational correlation time of the dye bound to the enzyme surface was observed, which suggested a depletion of cardiolipin layer due to complexation with the drug. The effect of Adriamycin on cardiolipin was drastic, leading to its phase separation. The present study suggests that the effect of Adriamycin on C*c*O is primarily a segregation of the cardiolipins.

Keywords: Time-resolved fluorescence; Adriamycin; 3,3′-Diethyloxadicarbocyanine iodide; Cytochrome *c* oxidase; Cardiolipin

* Corresponding author. Fax: +91-22-215-2110.
E-mail addresses: tdas@aecom.yu.edu (T. Kanti Das), shyamal@tifr.res.in (S. Mazumdar).

0301-4622/00/$ - see front matter
PII: S0301-4622(00)00158-7

1. Introduction

Cytochrome *c* oxidase (C*c*O) is the terminal respiratory enzyme and performs a key role in energy synthesis in the mitochondria [1,2]. C*c*O functions as a redox proton pump [3–5] that is coupled to the electron transfer process through a chain constituted of a homodinuclear copper center (Cu_A), heme *a*, and a binuclear center called heme a_3-Cu_B. Cytochrome *c* is the physiological electron donor that binds to C*c*O at a low ionic strength of the medium, and transfers electrons to Cu_A.

Bovine C*c*O contains 13 subunits. This multisubunit enzyme complex spans the inner mitochondrial membrane and remains in contact with the membrane phospholipids. The existence of a boundary of immobilized lipids between the hydrophobic protein surface and the adjacent fluid bilayer regions in bovine C*c*O was suggested by Jost et al. [6]. The number of membrane phospholipids that co-purify with C*c*O differs among various preparations. Commonly, bovine C*c*O contains 20–60 mol of phospholipid/mol of enzyme [7]. Some lipid-rich preparations of this enzyme, however, may have as many as 130 phospholipid molecules [8]. The major constituents of the lipids are phosphatidylethanolamine and phosphatidylcholine, which are easily extracted or exchanged by detergents [9–12]. However, some cardiolipins (diphosphatidylglycerol) bind tightly to the enzyme and are not easily extractable [7,13,14].

The enzymatic activity (electron transfer) of bovine C*c*O is greatly influenced by some of the surrounding boundary lipids [7,13,15]. Several studies have shown that the electron transport activity of C*c*O is diminished by 30–50% of its original activity when tightly bound cardiolipins are depleted from the enzyme when solubilized in non-ionic detergents [10,13,16]. The restoration of full enzyme activity can be achieved by the addition of cardiolipin, but not other phospholipids, to the cardiolipin-depleted enzyme [10,13,16,17]. However, the recovery of the enzyme activity has also been reported by the addition of other phospholipids to the cardiolipin-depleted enzyme [15,18,19]. Studies by Robinson et al. [20] suggested that out of 3–4 mol of tightly bound cardiolipin per aa_3 complex, at least two are required for full electron transport activity of the enzyme.

The crystal structure of bovine C*c*O shows the presence of eight bound phospholipids per monomer; five of them are phosphatidylethanolamine and three are phosphatidylglycerol [21]. The crystal form was obtained from an aqueous solution of the enzyme dissolved in a non-ionic detergent, decyl maltoside [22]. The lipids are located on the membrane surface of C*c*O in both the matrix and the cytosolic sides, but their hydrocarbon tails are directed toward the inside of the transmembrane region, as would be expected if these phospholipids were arranged in a lipid bilayer. Chemical analysis of the crystalline enzyme indicates the presence of only one equivalent of cardiolipin per monomer [23]. Although no cardiolipin was detected in their earlier crystal structure [21], it was suggested that some unassigned electron density in the inter-monomer space might arise from two cardiolipin molecules in the dimer. Recently, Yoshikawa [24] confirmed the presence of one cardiolipin per monomer in their refined structure.

The functional role of cardiolipin in controlling the activity of bovine C*c*O is unknown. The requirement of cardiolipin for C*c*O activity was proposed to be one of the causes of short-term

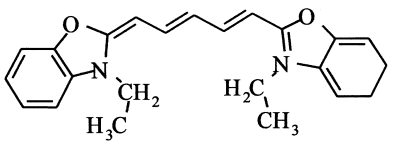

DODCI

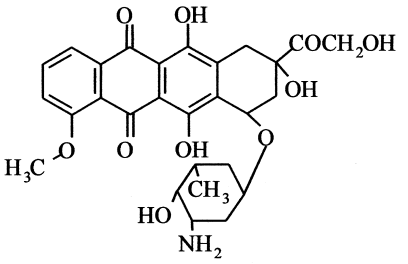

ADRIAMYCIN

Fig. 1. Chemical structure of Adriamycin and DODCI.

toxicity observed during treatment of patients with the anti-cancer drug, Adriamycin (Fig. 1) [25–29]. Adriamycin and its derivatives are among the most efficient antimitotics used in clinical therapy [30]. However, the cardiotoxicity induced by Adriamycin sets a crucial limit to the maximum dosage that may be administered, since the toxic effect is cumulative [25] and related to the impairment of mitochondrial functions [31]. The exact mechanism of Adriamycin-cardiomyopathy is not known. Several factors, including increased oxidative stress, the depression of antioxidants, tissue degradation by a free radical mechanism and the complex formation with cardiolipins in the inner mitochondrial membrane, have been suggested to contribute to Adriamycin-cardiotoxicity [30,32,33]. Although it is generally believed that the mechanism of inhibition of the cytochrome *c* oxidase activity by Adriamycin is a perturbation in the cardiolipin environment, very little is known about the effect of Adriamycin on the enzyme structure.

In the present work, a fluorescent dye, 3,3′-diethyloxadicarbocyanine iodide (DODCI) (Fig. 1) was used as a reporter for the lipid environment of C*c*O. We have studied the dynamics of the dye in C*c*O dissolved in lauryl maltoside by time-resolved fluorescence anisotropy. We also studied the dynamics in cardiolipin and asolectin dispersions. The changes in the rotational dynamics in C*c*O, cardiolipin and asolectin caused by Adriamycin were monitored. The findings of the present study support the model that the major effect of Adriamycin on C*c*O is a perturbation in the cardiolipin environment that causes significant structural changes in the enzyme.

2. Experimental procedures

2.1. Chemicals

Cardiolipin and asolectin (soybean phospholipid, type II-S) were purchased from Sigma (St. Louis, MO). The major composition of asolectin is made up of roughly equal proportions of phosphatidylethanolamine, phosphatidylcholine and phosphatidylinositol, and it was used after an acetone wash and drying. 3,3′-diethyloxadicarbocyanine iodide (DODCI) was purchased from Molecular Probes Inc. (Eugene, OR). Lauryl maltoside (LM) was a Fluka (Ronkonkoma, NY) product. Adriamycin hydrochloride was obtained from Farmitalia, Italy. Other reagents used were of the purest grade available commercially.

2.2. Purification of cytochrome c oxidase

Bovine C*c*O was extracted from beef heart following the method of Yonetani [34]. The pellets of C*c*O obtained following purification were dissolved in a lauryl maltoside solution (0.4%) in 100 mM phosphate buffer (pH 7.4). The purity of the isolated enzyme was checked by optical spectra and enzyme activity (electron transfer). The concentration of C*c*O was determined by using $\Delta\varepsilon$ (reduced minus oxidized = 25 mM^{-1} cm^{-1}) at 605 nm [35]. The electron transfer activity of C*c*O was ~ 160 s^{-1} at 25°C, pH 7.4 in 0.04% LM, measured by the loss of absorbance of ferrocytochrome *c*, monitored at 550 nm. Bovine C*c*O, isolated by Yoentani's method, usually contains less than 20 lipid molecules per monomer. The enzyme preparations were stored as small aliquots at -40°C.

2.3. Time-resolved fluorescence spectroscopy

The time-resolved fluorescence experiments were carried out using picosecond dye-laser pulses from a synchronously pumped cavity-dumped dye-laser (Rhodamine 6G) driven by the frequency-doubled output (532 nm) of a CW mode-locked Nd-YAG laser described elsewhere in detail [36]. Fluorescence decay curves were collected using a time-correlated single photon counting set-up coupled to a microchannel plate photomultiplier (Hamamatsu 2809). The width of the dye-laser pulse was ~ 4 ps and the half-width of the instrument response function was typically ~ 80 ps. The shortest fluorescence lifetimes that can be measured in this set-up are in the range of a few tens of ps. The excitation frequency for

recording DODCI (~ 0.4 μM) fluorescence decay was 574 nm, and the emission was recorded at 610 nm, except for DODCI in buffer alone, which was measured at 590 nm. Emission profiles were collected at the magic angle (54.7°) to eliminate any contribution from anisotropy decay. A Schott WG 590 nm cut-off filter was used to remove scattering from samples. To get the fluorescence decay curves, $1-3\times10^4$ counts were collected in the peak channel (total counts, $5-10\times10^5$). Each data set was collected in 512 channels and each channel width was 38 ps.

The observed fluorescence decay curves are the convolution of the excitation function and the fluorescence decay function. The deconvoluted fluorescence decay function (I) can be written as a sum of exponentials:

$$I(t)=\sum_k \alpha_k \exp(-t/\tau_k)\ k=1-4 \tag{1}$$

To get the amplitudes (α_k) and lifetimes (τ_k), an iterative reconvolution was applied using non-linear least squares regression by Marquardt's algorithm for parameter optimization. The goodness of an exponential fit was determined from the randomness of the weighted residuals distribution at a near-unity value of the reduced χ^2.

In the time-resolved anisotropy experiments, the polarized components of fluorescence components were collected after correcting for the geometry factor (G-factor) of the instrument [37]. The G-factor is defined as the ratio of the observed signals for the parallel and the perpendicular orientations of the polarizer when a depolarized emission source is kept in place of the sample. The G-factor-corrected data sets can be fitted with more reliability, because of a decrease in the number of fitting parameters due to a common scale factor for the parallel and the perpendicular decays. The G-factors at various emission wavelengths were determined by using cresyl violet as a standard. The G-factor correction in the anisotropy measurements was done by adjusting the collection time for the perpendicular component as a product of the G-factor and the collection time for the parallel component. The polarized fluorescence decays [$I_{//}(t)$, $I_{\perp}(t)$] were used to calculate the anisotropy decay function, *r(t)* [38], as given by:

$$\begin{aligned} I_{//}(t) &= \frac{1}{3}[1+2r(t)]I(t) \\ I_{\perp}(t) &= \frac{1}{3}[1-r(t)]I(t) \end{aligned} \tag{2}$$

where

$$I(t)=\Sigma_i \alpha_i \exp(-t/\tau_i)$$

and

$$r(t)=r_0\sum_i \beta_i \exp(-t/\phi_i) \tag{3}$$

where r_0 is the initial anisotropy, β_i is the pre-exponent ($\Sigma_i\beta_i=1$) and ϕ_i is the anisotropy decay constant. The goodness of the fits of the polarized decays to Eq. (2) was examined by the random distribution of the weighted residuals, reduced χ^2 value and a good match of the calculated anisotropy function to the experimental *r(t)*.

Steady-state fluorescence measurements (excitation wavelength = 574 nm) were performed using a Shimadzu RF540 spectrofluorimeter, and optical spectra were recorded by a Shimadzu UV-2100 spectrophotometer. All spectroscopic measurements were carried out at ~ 22°C.

3. Results

Fluorescent cyanine dyes have been widely used as a probe of various biophysical measurements in cells, organelles and vesicular systems [39–48]. These dyes are hydrophobic as well as cationic, and show an equilibrium distribution between the aqueous medium and the membrane [49,50]. Upon binding to the membrane phase, the cyanine dyes usually show a significant red-shift in the emission and absorption wavelengths. The use of a cyanine dye, DODCI (Fig. 1) in the present study is justified for several reasons. First, it can be used as a probe for the lipid environment of C*c*O, because of its relatively high affinity to lipids. Secondly, the fact that DODCI contains a positively charged

group suggests that the lipid-bound dye population will be sensitive to exogenously added ionic molecules (e.g. Adriamycin). Thirdly, the characteristics of its fluorescence lifetime and anisotropy in membranes and various micellar phases have been reported in great detail [37,50,51], which aid the understanding of the systems presently being studied.

3.1. Binding of DODCI to CcO-optical spectra

The absorption spectrum of pure DODCI in an aqueous medium shows a band at ~576 nm that shifts to 586 nm upon binding to C*c*O. The optical difference spectra were recorded as a function of the increasing concentration of DODCI to monitor the absorbance changes upon its binding with C*c*O (5 μM, 100 mM Tris buffer, 0.05% LM, pH 7.4). The association constant was calculated to be $\sim 4 \times 10^5$ M^{-1} from a double reciprocal plot [52] of the change in absorbance at 599 nm vs. the concentration of DODCI. This indicates a fairly strong binding of DODCI to C*c*O.

3.2. DODCI binding to lipids, detergents and CcO — fluorescence lifetimes

The steady state fluorescence spectrum of DODCI in aqueous solution shows an emission peak at ~590 nm. Upon the binding of DODCI to the lipids or the detergent used in the present study, the emission band is red-shifted to ~610 nm. The fluorescence decay of free DODCI (in aqueous buffer) follows single-exponential kinetics with a lifetime of 0.67 ns (Table 1), which matched with earlier reports [50]. DODCI in an aqueous vesicle (liposome) shows three lifetimes of 0.70, 1.71 and 0.12 ns, respectively (Table 1). The first lifetime is easily identified as arising from the dye population that is partitioned to the aqueous phase. The latter two were assigned to two membrane-bound populations of the dye [50]. A dye fraction that was embedded in the hydrophobic part of lipid showed the longest lifetime (1.71 ns), while the dye molecules that were in close interaction with the polar lipid head resulted in a short lifetime of 0.12 ns. Assignment of the lifetime components to the dye populations in different phases agreed with earlier reports [50,51]. Clearly, the different populations of DODCI that could be identified by their distinct lifetimes serve as reporters of the nature of the environment around them.

The lifetimes of DODCI in detergent and various lipids are presented in Table 1. The typical time-resolved decay of fluorescence values of DODCI in different solvent media are shown in Fig. 2. The partitioning of DODCI in LM was studied because LM is the detergent medium used to solubilize C*c*O in the present study. In

Table 1
Fluorescence lifetimes of DODCI in different environments

DODCI[a] (0.4 μM) in	τ_1[b] (ns)	α_1	τ_2 (ns)	α_2	τ_3 (ns)	α_3	χ^2
Phosphate buffer	0.67						1.01
Phosphate + Adriamycin (0.05 mg/ml)	0.68						1.12
Cardiolipin (0.06 mg/ml)	0.68	0.40	1.6	0.60			1.08
Cardiolipin + Adriamycin (0.05 mg/ml)	0.68	0.25	~0.2	0.75			1.15
LM (0.1%)	0.69	0.32	1.8	0.68			1.04
C*c*O (10 μM) in 0.1% LM	0.68	0.36	1.8	0.08	0.18	0.56	1.16
C*c*O, LM + Adriamycin (0.1 mg/ml)	0.68	0.53	1.8	0.06	0.18	0.41	1.19
Asolectin (0.1 mg/ml), 0.1% LM	0.68	0.15	1.8	0.85			1.08
Asolectin, LM + Adriamycin (0.1 mg/ml)	0.68	0.34	1.7	0.66			1.09
Liposome (0.11 mg/ml)[c]	0.70	0.51	1.71	0.23	0.12	0.26	1.19

[a] The buffer used in these measurements is 100 mM phosphate, pH 7.4.
[b] τ and α refer to lifetime and amplitude, respectively. The uncertainty in the values of τ and α is less than 5%.
[c] Liposomes were made by sonication of asolectin in 30 mM sodium phosphate, 150 mM NaCl, pH 7.5 [50].

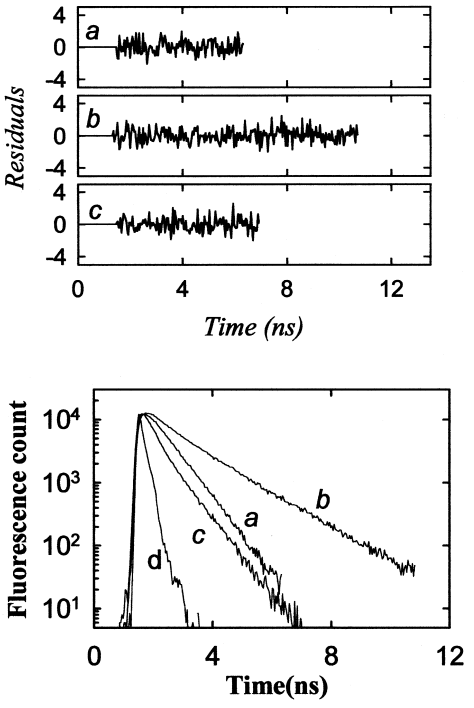

Fig. 2. Effect of Adriamycin on the fluorescence decay of DODCI in cardiolipin. Fluorescence decay of DODCI in: (a) phosphate buffer (100 mM), pH 7.4; (b) cardiolipin (0.06 mg/ml); (c) cardiolipin mixed with Adriamycin (0.05 mg/ml). The instrument response is shown in (*d*). In the top panel, the residuals for the corresponding decay curves are shown.

LM, DODCI shows only one bound-dye component with lifetime of 1.8 ns, and none with lifetime of 0.12 ns, indicating that the dye binds near the non-polar hydrocarbon chains. Asolectin that was dissolved in LM for better transparency of the solution shows only one bound-dye population. Cardiolipin was dispersed in aqueous buffer in the absence of detergent and without sonication to obtain reasonable clarity of the solution. Cardiolipin also shows a single bound-dye component (1.6 ns). Cardiolipin dispersed in LM also gave similar results. This is in contrast to the observations made with liposomes (made by sonication of asolectin in the absence of any detergent) described earlier where a second bound component (0.12 ns) is also detected [50]. It is to be noted here that no vesicle is formed when the lipids are dissolved in LM [37,51]. The major difference between liposomes and detergent-solubilized lipid is that the former has an ordered structure but the latter contains highly dynamic lipid–detergent mixed micellar aggregates [37,51].

In LM-solubilized C*c*O, DODCI shows two bound-dye populations (Table 1). The presence of the shorter lifetime component (0.18 ns) in a larger proportion (56%) relative to the longer lifetime component (1.8 ns, 8%) indicates that the dye binds preferentially to C*c*O rather than to the detergent. Hence, this shorter lifetime component (0.18 ns) serves as a useful probe to follow the structural changes in C*c*O.

3.3. Anisotropy decay of DODCI bound to CcO

Fluorescence anisotropy is related to the rotational dynamics of the emission dipole of the fluorophore. The time-resolved decay of fluorescence anisotropy is calculated using Eq. (2), from the decay of the parallel and perpendicular components of fluorescence emission of the dye as shown in Fig. 3. When a fluorophore exists in different environments exhibiting multiple fluorescence lifetimes, the anisotropy decay becomes complex due to the contributions from various components. In such systems, different fluorophore populations may show variation in their

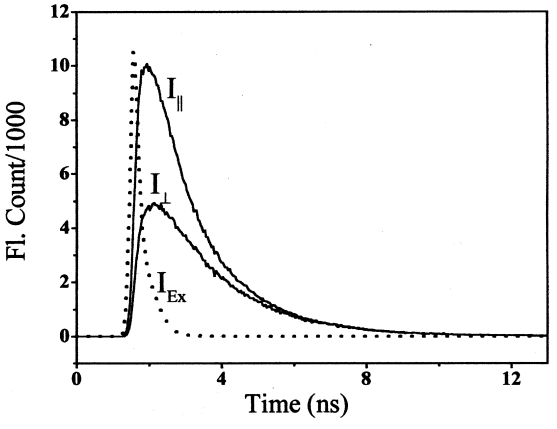

Fig. 3. The parallel and perpendicular components of time-resolved fluorescence decay of DODCI (0.4 μM) in: C*c*O (10 mM); 100 mM phosphate buffer; and 0.1% LM at pH 7.4. The time-resolved anisotropy decay [$r(t)$] was calculated using Eq. (2) from these results.

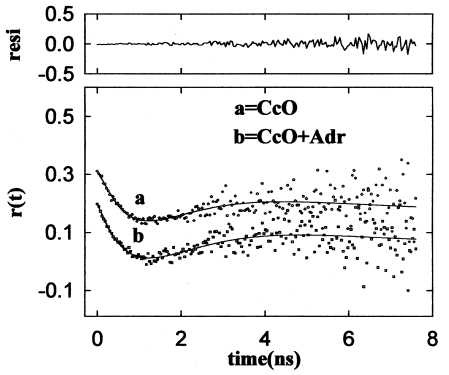

Fig. 4. Anisotropy decay of DODCI (0.4 μM) in: (a) C*c*O (10 μM, 100 mM phosphate buffer, 0.1% LM, pH 7.4); and (b) Adriamycin-treated C*c*O (0.1 mg/ml Adriamycin). The decay curve marked (b) is shifted down vertically for better clarity.

dynamic behavior, and hence the measured anisotropy decay has to be analyzed by a correct and physically meaningful model for the interpretation of data. Observation of unusual anisotropy decay was reported for fluorophores in lipid bilayers and lipid/proteins systems [53–55]. Such anisotropy decay curves have a peculiar 'dip and rise' shape that cannot be analyzed by a simple summation of multiple rotational correlation times (see Eq. (3)). The anisotropy decay of DODCI in C*c*O also shows an unusual 'dip and rise' shape (Fig. 4a). We have adopted the method of analysis proposed by Ludescher et al. [55], with some modifications, and tested it on the present case of DODCI-C*c*O. The basic features of the analysis are described below.

The observed anisotropy decay in the shorter time-scale is a weighted average of the anisotropies of all components. It is, therefore, necessary to use an associative model in which each dye population, characterized by a distinct fluorescence lifetime and anisotropy decay, contributes to the resultant anisotropy decay. After a sufficiently long time-scale, the rotational diffusion of only the species with long lifetimes contributes to the anisotropy decay. This situation arises in experiments with reasonably large biopolymers where the lifetimes of multiple fluorophore populations are significantly different. The time-dependent relative increase in the contribution from the long lifetime components may cause the anisotropy curve to rise or fall at long time-scale.

The time-dependent weighting factors are deduced as follows: for a fluorophore existing in multiple environments, the fluorescence decay, $I(t)$, can be expressed as:

$$I(t) = \sum_{i=1}^{n} \alpha_i I_i(t) \tag{4}$$

n being the total number of distinct environments and $\Sigma_i \alpha_i = 1$. The fractional intensity, $g_i(t)$, due to each component is given by:

$$g_i(t) = \frac{\alpha_i I_i(t)}{I(t)} \tag{5}$$

Fig. 5 shows plots of $g_i(t)$ for a three lifetime-component system. The fluorescence decay of DODCI in C*c*O was used as $I(t)$. It is obvious from the plots that the short lifetimes have a small contribution to $g_i(t)$ over longer periods of time, but they contribute maximally over a shorter time. The opposite is true for longer lifetimes.

In order to establish the significance of the time-dependent weight factors, we constructed several anisotropy decay curves as a function of $g_i(t)$. Values of $g_i(t)$ were calculated for various combinations of the fractional population of the fluorophore. The parameters used in the simulation are listed in Table 2. Fig. 6a shows the simulated anisotropy curves obtained by the variation of the two bound populations of DODCI

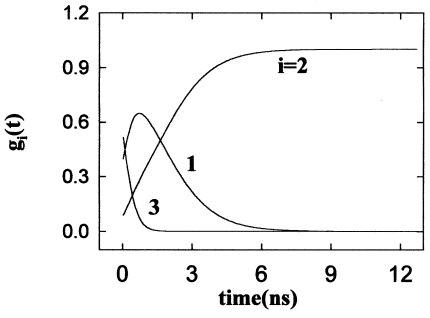

Fig. 5. Time-dependent weighting factors, $g_i(t)$, for a three-lifetime component system, calculated using Eq. (5). $i = 1$ ($\tau_1 = 0.68$ ns), $i = 2$ ($\tau_2 = 1.8$ ns), $i = 3$ ($\tau_3 = 0.18$ ns).

Table 2
The amplitude values (α) used in the simulations [using Eq. (9)] to construct the anisotropy curves shown in Fig. 6[a]

		Trace a	Trace b	Trace c	Trace d	Trace e	Trace f
Fig. 6a	α_1	0.37	0.37	0.37	0.37	0.37	0.37
	α_2	0.58	0.48	0.38	0.28	0.18	0.08
	α_3	0.05	0.15	0.25	0.35	0.45	0.55
Fig. 6b	α_1	0.00	0.03	0.11	0.21	0.29	0.37
	α_2	0.26	0.25	0.21	0.16	0.12	0.08
	α_3	0.74	0.72	0.68	0.63	0.59	0.55

[a] The fixed parameters are, $\tau_1 = 0.68$ ns, $\tau_2 = 1.8$ ns, $\tau_3 = 0.18$ ns, $\phi_1 = 0.58$, $\phi_2 = 4.9$, $\phi_3 = 5.0$, $\beta_2 = 0.40$, $\beta_3 = 0.95$.

keeping the free dye (0.68 ns) population (0.36) constant. It shows that the 'dip' in $r(t)$ decreases with an increasing population of the longer component (1.8 ns). However, the presence of a constant fraction of τ_1 (0.68 ns) maintains the 'dip and rise' nature of $r(t)$, even at the high population of the longer component (1.8 ns). Fig. 6b presents the decay curves constructed by varying the amplitudes of all of the three lifetime components (Table 2). For a small population of the short lifetime components, the 'dip and rise' feature almost vanishes. Hence, it is evident that the extent of 'dip and rise' is dependent on $g_i(t)$.

Here, we use $g_i(t)$ to derive an expression for analyzing the experimental anisotropy decay, $r(t)$. For a heterogeneous system, $r(t)$ is a linear combination of anisotropy decays from all species.

$$r(t) = \sum_{i=1}^{n} g_i(t) r_i(t) \tag{6}$$

and $r_i(t)$ can be written [56,57] as:

$$r_i(t) = r(0)\left[\beta_i \exp(-t/\phi_i) + (1-\beta_i)\exp(-t/\phi_p)\right] \tag{7}$$

where ϕ_i is the rotational correlation time of the fast internal motion of species i, β_i is the pre-exponential term and ϕ_p is the rotational correlation time of overall tumbling of the protein to which the dye is bound. β_i is a measure of the extent to which the emission is depolarized by each rotational component. It is related to the generalized order parameter [57], and is referred to here as the structure factor. Hence, $r(t)$ can be written as:

$$r(t) = r(0)\left[\sum_{i=1}^{n} g_i(t) \times \{\beta_i \exp(-t/\phi_i) + (1-\beta_i)\}\right] \times \exp(-t/\phi_p) \tag{8}$$

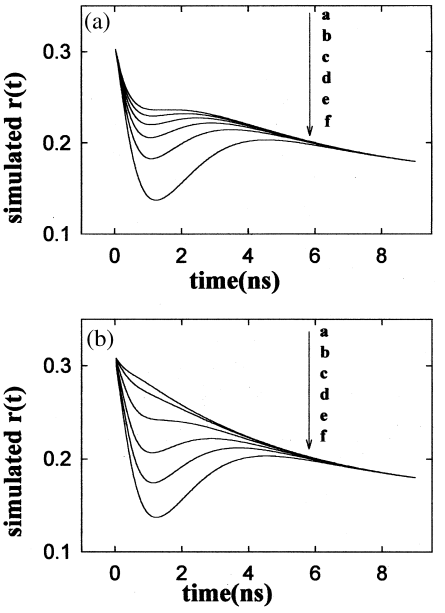

Fig. 6. Simulated anisotropy curves for a three-component system calculated using Eq. (9). (a) The amplitude of the first component (α_1) was kept constant and the remaining two were varied to generate the plots a–f. (b) All amplitudes were varied in the traces a–f. The amplitude values used in the simulation are listed in Table 2.

Table 3
Rotational correlation time of DODCI in different environments

A	ϕ_1 (ns)	ϕ_2 (ns)	β_2	ϕ_3 (ns)	β_3	$r_{2\infty}$	$r_{3\infty}$	r_0	χ^2
DODCI[a] in									
C*c*O in LM	0.58	4.9	0.40	5.0	0.95	0.186	0.015	0.31	1.21
C*c*O in LM + Adriamycin	0.54	5.2	0.44	1.6	0.96	0.170	0.012	0.30	1.20
B	ϕ_1 (ns)	β_1	ϕ_2 (ns)	β_2	r_0	χ^2			
DODCI[b] in									
Phosphate buffer	0.20					1.12			
LM	0.45	0.09	13	0.91	0.33	1.17			
Asolectin in LM	0.50	0.25	17	0.75	0.28	1.20			
Asolectin in LM + Adriamycin	0.48	0.22	18	0.78	0.30	1.22			
Cardiolipin	0.49	0.50	7	0.50	0.17	1.15			
Cardiolipin + Adriamycin	0.50				0.30	1.11			

[a] Data analyzed by fitting to Eq. (9). The uncertainties in the calculated values of ϕ, β and r are less than 10%. Sample conditions are the same as in Table 1.

[b] Data analyzed by fitting to Eq. (2). The uncertainties in the calculated values of ϕ, β and r are less than 10%. Sample conditions are the same as in Table 1.

If $\phi_p \gg \phi_i$, the $\exp(-t/\phi_p)$ term becomes close to unity. This is true for a dimer of C*c*O ($\sim$ 420 kDa), which by an empirical estimate (1 ns of rotational correlation time per 2400 Da mass) should give rise to a ϕ_p of $\sim$ 175 ns [58,59]. In the present case, another simplification is made noting that there is a component always present that corresponds to the free dye population. This component shows a rotational time of 0.2–0.5 ns in various media used in the present study (Table 3) and it is not expected to contribute to the residual anisotropy. Hence, $r(t)$ can be written for the present three lifetime components system as:

$$r(t) = r(0)\,[g_1(t)\exp(-t/\phi_1) + g_2(t)\{\beta_2\exp(-t/\phi_2) + (1-\beta_2)\} + g_3(t)\{\beta_3\exp(-t/\phi_3) + (1-\beta_3)\}] \quad (9)$$

where $r_0(1-\beta_i) = r_{i\infty}$, the residual anisotropy of the ith component. The non-zero values of $r_{i\infty}$ arise from restricted motion of the bound dye.

The experimental anisotropy curves of DODCI in C*c*O could be successfully fitted to Eq. (9) to extract the rotational parameters. A fit to the experimental anisotropy decay of DODCI in C*c*O is shown as a solid line in Fig. 4a. The distribution of residuals for this fit is plotted in the topmost trace of Fig. 4 showing the goodness of the fit. The rotational correlation times (ϕ_i), the residual anisotropies ($r_{i\infty}$) and the structure factors (β_i) recovered from the fit are listed in Table 3a. ϕ_1 corresponds to the motion of the dye in aqueous phase. DODCI in aqueous buffer (100 mM phosphate, pH 7.4) has a rotation time of 0.2 ns (Table 3b). However, in the presence of detergents/lipids, the motion of the 'free' dye becomes slower ($\sim$ 0.5 ns) due to an increase in the viscosity of the medium and also possibly due to weak interactions with the surfactant monomers. The motion of the dye molecules bound to C*c*O experiences retardation and shows a much longer rotational time. Both of the bound-dye components show the same rotational time ($\phi_2 = 4.9$ ns, $\phi_3 = 5$ ns) that possibly corresponds to local motions of the dye bound to the protein. Global motion of this large protein is expected to be much slower. Although the two bound dye populations have similar values of ϕ_2 and ϕ_3, they show a large difference in the values of residual anisotropy and structure factor. One of them ($\tau_2 = 1.8$ ns, $\phi_2 = 4.9$ ns) shows a large residual anisotropy ($r_{2\infty} = 0.18$) as well as a small value for the structure factor ($\beta_2 = 0.4$) suggesting that this

dye population experiences hindered rotation. This is further consistent with our earlier proposal that the longer lifetime (1.8 ns) arises from the dye buried in the hydrophobic phase. The other population of the bound dye ($\tau_3 = 0.18$ ns, $\phi_3 = 5$ ns) shows a small residual anisotropy ($r_{3\infty} = 0.015$) and a near-unity value for the structure factor ($\beta_3 = 0.95$), indicating less hindrance in rotation of these dye molecules. As discussed earlier, this population corresponds to the dye molecules strictly bound to C*c*O. Analysis of the anisotropy decay data with a non-associative model did not give any consistent or physically meaningful parameters, indicating that the fluorescence dynamics of the dye molecules in the present case involves the partitioning of the dye in different phases, in which both the lifetime and the associated fluorescence depolarization dynamics were modulated.

3.4. Effect of Adriamycin on CcO

Upon the addition of Adriamycin to C*c*O, the lifetimes of the DODCI fluorescence remained unchanged. However, the amplitudes of τ_1 and τ_3 (0.67 ns and 0.18 ns, respectively, see Table 1) show appreciable changes, whereas that of τ_2 (1.8 ns) remains almost the same (Table 1). This suggests that the population of the dye bound to the enzyme phase decreases and the population in aqueous phase increases on addition of Adriamycin. This indicates that Adriamycin probably interacts with the lipids of C*c*O, which is consistent with earlier studies [26–29]. For a better understanding of the effect of Adriamycin on the lipids of C*c*O, we studied the interaction of Adriamycin with asolectin and cardiolipin. Adriamycin does not affect the lifetime of DODCI in aqueous buffer (Table 1). Upon the addition of Adriamycin to asolectin, a significant portion of the bound-dye was released into the aqueous phase. The effect of Adriamycin on cardiolipin was rather drastic, as shown in Fig. 2. The fluorescence decay of DODCI in aqueous buffer is shown in trace (a) of Fig. 2. Upon binding to cardiolipin, the decay time became significantly longer (trace b), which is consistent with the appearance of the 1.6 ns lifetime. When Adriamycin was added, a strong quenching was observed (trace c), and the analysis shows that the whole population of the bound dye (1.6 ns) disappeared. Instead, a short lifetime (~ 0.2 ns) was observed, probably due to the dyes bound to the Adriamycin–cardiolipin complex. It is to be noted that the determination of a precise value of this lifetime was difficult to obtain because of high scattering from the complex. Eventually, the cardiolipin–Adriamycin complex was separated from the solution phase. Thus ,it is evident that the effect of Adriamycin was much stronger on cardiolipin than on other phospholipids, and this is consistent with an earlier report that the affinity of Adriamycin for cardiolipin is ~ 80 times higher than that for phosphatidic acid [26]. The above discussions bolster our suggestion that Adriamycin affects cardiolipin as well as other phospholipids bound to C*c*O.

To assess the changes in the structural dynamics of C*c*O and the lipids caused by Adriamycin, we determined the rotational correlation times from anisotropy data (Table 3). The polarized fluorescence of DODCI in LM and in the lipids was satisfactorily fitted to Eq. (2). The values of ϕ_1 (~ 0.5 ns) in Table 3 represent the rotational time of the dye in the aqueous phase, as mentioned earlier. ϕ_2 represents the global motion of the detergent micelles (LM), or the lipid-detergent aggregates (Table 3b) [37,51]. A rotational correlation time of 13 ns for LM suggests that it forms relatively large micelles with an estimated aggregation number of > 60 (under the present experimental conditions). An increase in ϕ_2 in asolectin–LM is consistent with the formation of lipid–micelle aggregates. When Adriamycin was added to asolectin, the observed change in the rotational correlation time (ϕ_2) of the bound dye was insignificant, suggesting that Adriamycin does not perturb the phospholipid structure. On the other hand, the complexation of Adriamycin with cardiolipin resulted in a complete disappearance of ϕ_2 (7 ns). The rotational correlation time of the Adriamycin–cardiolipin complex could not be determined because the complex precipitated.

When C*c*O is treated with Adriamycin (Fig. 4b), the rotational correlation time of one of the

two bound-dye components (ϕ_3) shows a significant change (from 5 to 1.6 ns). The other rotational time (ϕ_2) does not show any significant change. The decrease in ϕ_3 is much larger than the uncertainties associated with the data (Fig. 4, Table 3a). This population of the bound dye is represented by the lifetime component τ_3 (0.18 ns) that has been shown in the previous section to be specifically bound to C*c*O. Moreover, the amplitude of this lifetime component decreased significantly upon Adriamycin treatment. The decrease in ϕ_3 indicates an increased mobility of the surface-bound dyes due to the effect of Adriamycin. This is best explained by the dissociation of a fraction of the lipids containing the dye from the protein and/or a significant perturbation of the lipid environment.

4. Discussions

The fluorescence dynamics data presented in this paper clearly suggest that the structural changes in cardiolipin and cytochrome *c* oxidase affected by Adriamycin can be detected. The drastic effect of Adriamycin on cardiolipin that was observed here is consistent with a sequestering of the cardiolipin molecules. Thus, our studies are in good agreement with the models proposed by others that describe Adriamycin-induced cardiotoxicity in terms of a segregation of cardiolipins [30]. Our results also show that Adriamycin indeed has some interaction with other phospholipids indicated by a significant change in the population of the bound-dye component (Table 1). However, the fact that neither the lifetime nor the rotational dynamics of the asolectin-bound dye show any appreciable change upon treatment with Adriamycin suggests that the phospholipids in asolectin are neither phase-separated nor form a strong complex with Adriamycin. Thus, the interaction of Adriamycin with the phospholipids in asolectin is much weaker than that with cardiolipin. In C*c*O, a significant decrease of the bound dye population upon addition of Adriamycin suggests that the lipids of C*c*O indeed interact with Adriamycin. Among these lipids, only cardiolipin is probably segregated from the protein, which is manifested by a large decrease in the rotational time of the C*c*O-bound dye (Table 3a).

The interaction of Adriamycin with the lipids is likely to be electrostatic in nature. In C*c*O, the phospholipids are attached to the protein surface by salt bridges and/or hydrogen bond interactions between their polar head groups and the amino acid side chains, the main chain imides, or the carbonyl groups [21]. They are also stabilized by hydrophobic interactions between the nonpolar lipid tails and the hydrophobic amino acid residues in the transmembrane region. The positively charged Adriamycin molecules are likely to weaken the salt bridges and the hydrogen-bonding, thus decreasing the stabilization energy of lipid-binding. Negatively charged lipids would be affected the most in comparison to the neutral lipids. This is consistent with an earlier report that the neutral lipid DPPC (dipalmitoylphosphatidylcholine) shows no association with Adriamycin [30]. Among the negatively charged lipids, cardiolipin has the highest affinity (association constant of $1.6 \times 10^6\ M^{-1}$) to bind Adriamycin. The higher affinity of cardiolipin, relative to the other negatively charged phospholipids, has been proposed to be the result of the stacking of the neighboring anthraquinone planes in a 2:4 cardiolipin–Adriamycin complex that imparts some additional stabilization energy [30].

We now address the question of how C*c*O is inactivated by Adriamycin. It is known that cardiolipin has a definite role in maintaining the original enzyme activity. However, the mechanism by which cardiolipin acts to influence enzyme activity is poorly understood. Proposals have been made that cardiolipin may perturb the conformation of the enzyme that facilitates the electron transfer from cytochrome *c* [20]. It also has been proposed that C*c*O exists in two conformations; cardiolipin facilitates interconversion between them and also causes an electrostatic enhancement of the surface concentrations of both cytochrome *c* and protons [17]. However, none of the proposals presented to date explains the cardiolipin effect satisfactorily. The structural model of Yoshikawa [23,24] suggests that cardiolipin may play a role in stabilizing the dimer structure. Thus, it seems

that monomers are formed in the cardiolipin-depleted enzyme. However, it is not known whether the enzyme activity comes only from the dimers and not from the monomers. Although an exact mechanism of the control of electron transfer by cardiolipin is not known, it has been established that cardiolipin binds the oxidase specifically and influences the electron transfer rate. The structural effect of Adriamycin on C*c*O may be reconciled with the cardiolipin effect on activity, which implies that the inactivation of C*c*O by Adriamycin occurs primarily due to a sequestering of cardiolipins.

The cardiotoxic effect of Adriamycin, however, is not limited to the inactivation of C*c*O. There are other membrane-proteins in the electron transport chain, e.g. complex I, complex III and glycerol-3-phosphate dehydrogenase, that require cardiolipin for their maximum electron transport activity [60–63]. Adriamycin is known to inhibit complex I and complex III [61]. Thus, it appears that the general mechanism of inhibition of the electron transport chain by Adriamycin is through an interaction with cardiolipin, a phospholipid specific to the inner mitochondrial membrane.

Acknowledgements

This work was supported by the Tata Institute of Fundamental Research.

References

[1] G.T. Babcock, M. Wikstrom, Oxygen activation and the conservation of energy in cell respiration, Nature 356 (1992) 301–309.
[2] H. Michel, J. Behr, A. Harrenga, A. Kannt, Cytochrome *c* oxidase: structure and spectroscopy, Annu. Rev. Biophys. Biomol. Struct. 27 (1998) 329–356.
[3] R.B. Gennis, Multiple proton-conducting pathways in cytochrome oxidase and a proposed role for the active-site tyrosine, Biochim. Biophys. Acta 1365 (1998) 241–248.
[4] M. Wikstrom, J.E. Morgan, M.I. Verkhovsky, On the mechanism of proton translocation by respiratory enzyme, J. Bioenerg. Biomembr. 30 (1998) 139–145.
[5] P.R. Rich, S. Junemann, B. Meunier, Protonmotive mechanism of heme-copper oxidases, J. Bioenerg. Biomembr. 30 (1998) 131–138.
[6] P.C. Jost, O.H. Griffith, R.A. Capaldi, G. Vanderkooi, Evidence for boundary lipid in membranes, Proc. Natl. Acad. Sci. USA 70 (1973) 480–484.
[7] N.C. Robinson, J. Zborowski, L.H. Talbert, Cardiolipin-depleted bovine heart cytochrome c oxidase: binding stoichiometry and affinity for cardiolipin derivatives, Biochemistry 29 (1990) 8962–8969.
[8] A. Seelig, J. Seelig, Phospholipid composition and organization of cytochrome c oxidase preparations as determined by 31P-nuclear magnetic resonance, Biochim. Biophys. Acta. 815 (1985) 153–158.
[9] N.C. Robinson, R.A. Capaldi, Interaction of detergents with cytochrome *c* oxidase, Biochemistry 16 (1977) 375–381.
[10] N.C. Robinson, F. Strey, L. Talbert, Investigation of the essential boundary layer phospholipids of cytochrome c oxidase using Triton X-100 delipidation, Biochemistry 19 (1980) 3656–3661.
[11] C. Yu, L. Yu, T.E. King, Studies on cytochrome oxidase. Interactions of the cytochrome oxidase protein with phospholipids and cytochrome *c*, J. Biol. Chem. 250 (1975) 1383–1392.
[12] S.B. Vik, R.A. Capaldi, Lipid requirements for cytochrome *c* oxidase activity, Biochemistry 16 (1977) 5755–5759.
[13] N.C. Robinson, Specificity and binding affinity of phospholipids to the high-affinity cardiolipin sites of beef heart cytochrome *c* oxidase, Biochemistry 21 (1982) 184–188.
[14] M.B. Cable, G.L. Powell, Spin-labeled cardiolipin: preferential segregation in the boundary layer of cytochrome *c* oxidase, Biochemistry 19 (1980) 5679–5686.
[15] S.B. Vik, G. Georgevich, R.A. Capaldi, Diphosphatidylglycerol is required for optimal activity of beef heart cytochrome *c* oxidase, Proc. Natl. Acad. Sci. USA 78 (1981) 1456–1460.
[16] M.P. Dale, N.C. Robinson, Synthesis of cardiolipin derivatives with protection of the free hydroxyl: its application to the study of cardiolipin stimulation of cytochrome *c* oxidase, Biochemistry 27 (1988) 8270–8275.
[17] D.A. Abramovitch, D. Marsh, G.L. Powell, Activation of beef-heart cytochrome c oxidase by cardiolipin and analogues of cardiolipin, Biochim. Biophys. Acta 1020 (1990) 34–42.
[18] Y.C. Awasthi, T.F. Chuang, T.W. Keenan, F.L. Crane, Tightly bound cardiolipin in cytochrome oxidase, Biochim. Biophys. Acta 226 (1971) 42–52.
[19] M. Fry, D.E. Green, Cardiolipin requirement by cytochrome oxidase and the catalytic role of phospholipid, Biochem. Biophys. Res. Commun. 93 (1980) 1238–1246.
[20] N.C. Robinson, Functional binding of cardiolipin to cytochrome *c* oxidase, J. Bioenerg. Biomembr. 25 (1993) 153–163.
[21] T. Tsukihara, H. Aoyama, E. Yamashita, T. Tomizaki, H. Yamaguchi, K. Shinzawa-Itoh, R. Nakashima, R. Yaono, S. Yoshikawa, The whole structure of the 13-

subunit oxidized cytochrome *c* oxidase at 2.8 A, Science 272 (1996) 1136–1144.
[22] T. Tsukihara, H. Aoyama, E. Yamashita, T. Tomizaki, H. Yamaguchi, K. Shinzawa-Itoh, R. Nakashima, R. Yaono, S. Yoshikawa, Structures of metal sites of oxidized bovine heart cytochrome *c* oxidase at 2.8 A, Science 269 (1995) 1069–1074.
[23] S. Yoshikawa, K. Shinzawa-Itoh, T. Tsukihara, Crystal structure of bovine heart cytochrome *c* oxidase at 2.8 A resolution, J. Bioenerg. Biomembr. 30 (1998) 7–14.
[24] S. Yoshikawa, Tenth European Bioenergetics Conference, June, Göteborg, Sweden, 1998.
[25] R.A. Minow, R.S. Benjamin, E.T. Lee, J.A. Gottlieb, Adriamycin cardiomyopathy-risk factors, Cancer 39 (1977) 1397–1402.
[26] E. Goormaghtigh, R. Brasseur, J.M. Ruysschaert, Adriamycin inactivates cytochrome *c* oxidase by exclusion of the enzyme from its cardiolipin essential environment, Biochem. Biophys. Res. Commun. 104 (1982) 314–320.
[27] E. Goormaghtigh, J.M. Ruysschaert, Anthracycline glycoside-membrane interactions, Biochim. Biophys. Acta. 779 (1984) 271–288.
[28] E.J.F. Demant, Inactivation of cytochrome *c* oxidase activity in mitochondrial membranes during redox cycling of doxorubicin, Biochem. Pharmacol. 41 (1991) 543–552.
[29] B.B. Hasinoff, J.P. Davey, Adriamycin and its iron(III) and copper(II) complexes. Glutathione-induced dissociation; cytochrome *c* oxidase inactivation and protection; binding to cardiolipin, Biochem. Pharmacol. 37 (1988) 3663–3669.
[30] E. Goormaghtigh, P. Huart, M. Praet, R. Brasseur, J.M. Ruysschaert, Structure of the Adriamycin-cardiolipin complex. Role in mitochondrial toxicity, Biophys. Chem. 35 (1990) 247–257.
[31] E. Bachmann, E. Weber, G. Zbinden, Effects of seven anthracycline antibiotics on electrocardiogram and mitochondrial function of rat hearts, Agents Actions 5 (1975) 383–393.
[32] X. Yin, H. Wu, Y. Chen, Y.J. Kang, Induction of antioxidants by Adriamycin in mouse heart, Biochem. Pharmacol. 56 (1988) 87–93.
[33] P.K. Singal, N. Iliskovic, T. Li, D. Kumar, Adriamycin cardiomyopathy: pathophysiology and prevention, Fed. Am. Soc. Exp. Biol. J. 11 (1997) 931–936.
[34] T. Yonetani, Cytochrome oxidase from beef heart muscle, Biochem. Prep. 11 (1966) 14–20.
[35] N. Sone, P. Nicholls, Effect of heat treatment on oxidase activity and proton-pumping capability of proteoliposome-incorporated beef heart cytochrome *aa*3, Biochemistry 23 (1984) 6550–6554.
[36] N. Periasamy, S. Doraiswamy, G.B. Maiya, B. Venkataraman, Diffusion controlled reactions: fluorescence quenching of cationic dyes by charge quenchers, J. Chem. Phys. 88 (1988) 1638–1651.
[37] T.K. Das, Rotational dynamics of lipid/detergent mixture: a mechanism for membrane protein reconstitution into lipid vesicles, J. Phys. Chem. 100 (1996) 20143–20147.
[38] R.F. Steiner, Fluorescence anisotropy: theory and applications, in: J.R. Lakowicz (Ed.), Topics in Fluorescence Spectroscopy, vol. 2, Plenum, New York, 1991, pp. 1–52.
[39] A. Waggoner, Optical probes of membrane potential, J. Membr. Biol. 27 (1976) 317–334.
[40] A.S. Waggoner, C.H. Wang, R.L. Tolles, Mechanism of potential-dependent light absorption changes of lipid bilayer membranes in the presence of cyanine and oxonol dyes, J. Membr. Biol. 33 (1977) 109–140.
[41] A.P. Singh, P. Nicholls, Cyanine and safranine dyes as membrane potential probes in cytochrome *c* oxidase reconstituted proteoliposomes, J. Biochem. Biophys. Methods 11 (1985) 95–108.
[42] M. Reers, T.W. Smith, L.B. Chen, J-aggregate formation of a carbocyanine as a quantitative fluorescent indicator of membrane potential, Biochemistry 30 (1991) 4480–4486.
[43] G. Cabrini, A.S. Verkman, Mechanism of interaction of the cyanine dye diS-C3-(5) with renal brush-border vesicles, J. Membr. Biol. 90 (1990) 163–175.
[44] U. Kragh-Hansen, K.E. Jorgensen, M.I. Sheikh, The use of a potential-sensitive cyanine dye for studying ion-dependent electrogenic renal transport of organic solutes. Uptake of L-malate and D-malate by luminal-membrane vesicles, Biochem. J. 208 (1982) 369–376.
[45] A.R. Oseroff, D. Ohuoha, G. Ara, D. McAuliffe, J. Foley, L. Cincotta, Intramitochondrial dyes allow selective in vitro photolysis of carcinoma cells, Proc. Natl. Acad. Sci. USA 83 (1986) 9729–9733.
[46] D. Yoshikami, L.M. Okun, Staining of living presynaptic nerve terminals with selective fluorescent dyes, Nature 310 (1984) 53–56.
[47] J.C. Smith, Potential-sensitive molecular probes in membranes of bioenergetic relevance, Biochim. Biophys. Acta 1016 (1990) 1–28.
[48] J.C. Freedman, T.S. Novak, Optical measurement of membrane potential in cells, organelles, and vesicles, Methods Enzymol. 172 (1990) 102–122.
[49] B. Ehrenberg, V. Montana, M.D. Wei, J.P. Wuskell, L.M. Loew, Membrane potential can be determined in individual cells from the nernstian distribution of cationic dyes, Biophys. J. 53 (1988) 785–794.
[50] T.K. Das, N. Periasamy, G. Krishnamoorthy, Mechanism of response of potential-sensitive dyes studied by time-resolved fluorescence, Biophys. J. 64 (1993) 1122–1132.
[51] T.K. Das, Rotational dynamics of lipid-detergent mixtures probed by a cyanine dye: A mechanism for vesicle formation, J. Chem. Soc. Faraday Trans. 92 (1996) 4279–4283.
[52] A. Schejter, A. Lanir, N. Epstein, Binding of hydrogen donors to horseradish peroxidase: a spectroscopic study, Arch. Biochem. Biophys. 174 (1976) 36–44.
[53] P.K. Wolber, B.S. Hudson, Bilayer acyl chain dynamics and lipid-protein interaction: the effect of the M13 bacteriophage coat protein on the decay of the fluores-

cence anisotropy of parinaric acid, Biophys. J. 37 (1982) 253–262.

[54] C.R. Guest, R.A. Hochstrasser, C.G. Dupuy, D.J. Allen, S.J. Benkovic, D.P. Millar, Interaction of DNA with the Klenow fragment of DNA polymerase I studied by time-resolved fluorescence spectroscopy, Biochemistry 30 (1991) 8759–8770.

[55] R.D. Ludescher, L. Peting, S. Hudson, B. Hudson, Time-resolved fluorescence anisotropy for systems with lifetime and dynamic heterogeneity, Biophys. Chem. 28 (1987) 59–75.

[56] K. Kinosita, S. Kawato, A. Ikegami, A theory of fluorescence polarization decay in membranes, Biophys. J. 20 (1977) 289–305.

[57] G. Lipari, A. Szabo, Effect of librational motion on fluorescence depolarization and nuclear magnetic resonance relaxation in macromolecules and membranes, Biophys. J. 30 (1980) 489–506.

[58] T.K. Das, S. Mazumdar, Conformational substrates of apoprotein of horseradish peroxidase in aqueous solution: a fluorescence dynamics study, J. Phys. Chem. 99 (1995) 13283–13290.

[59] J.E. Brunet, V. Vargas, E. Gratton, D.M. Jameson, Hydrodynamics of horseradish peroxidase revealed by global analysis of multiple fluorescence probes, Biophys. J. 66 (1994) 446–453.

[60] M. Fry, D.E. Green, Cardiolipin requirement for electron transfer in complex I and III of the mitochondrial respiratory chain, J. Biol. Chem. 256 (1981) 1874–1880.

[61] E. Goormaghtigh, P. Huart, R. Brasseur, J.M. Ruysschaert, Mechanism of inhibition of mitochondrial enzymatic complex I–III by Adriamycin derivatives, Biochim. Biophys. Acta 861 (1986) 83–94.

[62] K. Nicolay, B. de Kruijff, Effects of Adriamycin on respiratory chain activities in mitochondria from rat liver, rat heart and bovine heart. Evidence for a preferential inhibition of complex III and IV, Biochim. Biophys. Acta 892 (1987) 320–330.

[63] Z. Beleznai, V. Jancsik, Role of cardiolipin in the functioning of mitochondrial L-glycerol-3-phosphate dehydrogenase, Biochem. Biophys. Res. Commun. 159 (1989) 132–139.